Mechanical Systems and Signal Processing ▮ (▮▮▮▮) ▮▮▮–▮▮▮

Contents lists available at ScienceDirect

Mechanical Systems and Signal Processing

journal homepage: www.elsevier.com/locate/jnlabr/ymssp

Design of piezo-based AVC system for machine tool applications

F. Aggogeri [a], F. Al-Bender [b], B. Brunner [c], M. Elsaid [b], M. Mazzola [a,*], A. Merlo [d], D. Ricciardi [d], M. de la O Rodriguez [e], E. Salvi [d]

[a] Department of Mechanical and Industrial Engineering, University of Brescia, Via Branze, 38, 25123 Brescia, Italy
[b] Katholieke Universitiet Leuven – PMA Div., Celestijnenlaan 300B, BE-3001 Heverlee, Belgium
[c] Fraunhofer-Institut für Silicatforschung ISC, Neunerplatz, 2, D-97082 Würzburg, Germany
[d] CE.S.I. Centro Studi Industriali, Via Tintoretto 10, 20093 Cologno M.se, Italy
[e] Fundación Tecnalia Research & Innovation, Paseo Mikeletegi, 7 - Parque Tecnológico, E-20009 San Sebastian, Spain

ARTICLE INFO

Article history:
Received 2 February 2011
Received in revised form
28 May 2011
Accepted 8 June 2011

Keywords:
Piezoelectric stack actuator
Active vibration control
Machine tool
Robust design

ABSTRACT

The goal of machine tools for Ultra High Precision Machining is to guarantee high specified performances and to maintain them over life cycle time. In this paper the design of an innovative mechatronic subsystem (platform) for Active Vibration Control (AVC) of Ultra High Precision micromilling Machines is presented. The platform integrates piezoelectric stack actuators and a novel sensor concept. During the machining process (e.g. milling), the contact between the cutting tool and the workpiece surface at the tool tip point generates chattering vibrations. Any vibration is recorded on the workpiece surface, directly affecting its roughness. Consequently, uncontrolled vibrations lead to poor surface finishing, unacceptable in high precision milling. The proposed Smart Platform aims to improve the surface finishing of the workpiece exploiting a broadband AVC strategy. The paper describes the steps throughout the design phase of the platform, beginning from the actuator/sensor criteria selection taking into account both performance and durability. The novel actuation principle and mechanism and the related FE analysis are also presented. Finally, an integrated mechatronic model able to predict in closed-loop the active damping and vibration-suppression capability of the integrated system is presented and simulation results are discussed.

1. Introduction

The design of innovative machine tools reflects the behaviour of the modern markets, where the customer's expectations have dramatically increased. Many researches aim to apply innovative solutions to obtain high machining performances and quality of products, reducing the life cycle cost at the same time. The manufacturers want to purchase machines with high flexibility, high accuracy, high modularity and high reliability. In particular, micromachining excellence implies innovative solutions able to perform dimension-constrained extremely precise works and to maintain these performances over time. Thus the robust design of systems integrated in a machine tool has to find solutions to solve the problems and to increase the performance of the micromachining processes.

During manufacturing processes performed by machine tools, the spindle is subjected to vibrations. Such vibrations can be classified as forced or self-excited (chatter). Due to the machine processing or transmitted through the foundation from

* Corresponding author. Tel.: +39 0303715578; fax: +39 0303702448.
E-mail address: marco.mazzola@ing.unibs.it (M. Mazzola).

0888-3270/$ - see front matter © 2011 Elsevier Ltd. All rights reserved.
doi:10.1016/j.ymssp.2011.06.012

Nomenclature

a	coefficient of Black's equation (cycles∗m/V)
A_f	accelerating factor
B_x	time equivalent to x% unreliability
d	piezoelectric d-constant (C/N)
D	electric density or flux density (C/m^2)
$f(t)$	probability density function of time t
E	applied electric field (V/m)
E_{ac}	activation energy (eV)
F	vector of forces
F_{pzt}	the actuation force
k	Boltzmann's constant (eV/K)
$[K]$	stiffness matrix
k_a	stiffness of the piezoceramic stack
K_c	solution of the CARE equation
K_e	solution of the FARE equation
L	mechanical stress (N/m^2)
$[M]$	positive definite mass matrix
$MTTF$	mean time to failure (h, cycles)
n	coefficient of Black's equation
Q_{pzt}	charge of the piezo stack
s	mechanical compliance (inverse of Young's modulus) (m^2/N)
SM	safety margin
S	mechanical strain (m/m)
t	time (or cycles)
T	absolute temperature (K)
u	force input vector
v_u	process noise
v_y	measurement noise
$[V]$	symmetric damping matrix
V_{max}	maximum voltage allowed
V_{pzt}	voltage applied to the piezo stack
w^T	exogenous input
x	state vector
x_{pzt}	stroke of the piezo stack
y	measured output (signals from the sensor)
z	vector of displacements
β	shape parameter of the Weibull distribution
Γ	gamma function
ε	dielectric permittivity of the material (C^2/N m^2)
η	scale parameter of the Weibull distribution
λ	parameter of the exponential distribution
$\lambda(t)$	failure rate function
μ_P	mean of preload (MPa)

other machines, the vibrations are often encountered and difficult to avoid. However, they represent a known problem and different methods can be applied to reduce, or even eliminate, their effect as soon as the sources have been identified.

Unbalanced effects, gear and bearing irregularities, multi-tooth cutter impact as well as the motion of the foundation induce forced vibrations. In contrast, chatter is a basic (or self-excited) instability of the cutting mechanism. The chatter vibration is not induced by external periodic forces, but the forces causing and maintaining it are generated during the vibratory process itself (the dynamic cutting process). Machine tool chatter vibrations depend on a self-excitation mechanism in the generation of chip thickness during machining operations [1,2]. Whatever the source, the vibratory motion affects the cutting process, because the tool and the workpiece are not constantly in contact. Any vibratory motion at the tool tip point between the cutting tool and the workpiece increases the roughness, thus the surface finishing could be unsatisfactory, affecting the quality of the product.

The Smart Platform (hereafter SP) is an active machine element intended to solve this problem that is particularly felt by micromachining producers and users. This innovative system is designed to limit the relative motion between the tool and the workpiece. In practice, the idea behind the SP is to filter the vibratory motion by directly controlling the position of the tool-spindle (or that of the table where the workpiece is placed).

The state of the art under piezo-based AVC solutions shows some applications to traditional turning and milling processes [3–6]. The application of this kind of devices to micromilling machines represents a real innovation. Furthermore, the SP improved in intrinsic mechanical stiffness and system compactness. Moreover, in order to widen the applicability and increase the flexibility and the modularity of the SP, the authors realise an Active Vibration Control system. The integrated system is configurable in two versions by changing the element responsible for the vibration compensation: the Adaptronic Spindle Platform where the spindle is connected to the flange of the ram by a mobile platform compensating the vibration (like a Sky-hook system) and the Adaptronic Table where the workpiece is moved to effect the compensation.

The paper shows the steps of the robust design process of the SP, by considering the mechatronic, the control and the durability performance as a whole. In the following section, the design principles of the SP are discussed. Section 3 outlines the mechatronics design aspects and the control methodology.

2. Smart Platform: principles and design

The integrated system presented in this paper aims to improve the surface finishing of the workpiece through a broadband AVC device based on high performance piezoelectric actuators.

Since the vibration is actively controlled, the actuation system is the key element to be considered from the early design stage.

Please cite this article as: F. Aggogeri, et al., Design of piezo-based AVC system for machine tool applications, Mechanical Systems and Signal Processing (2011), doi:10.1016/j.ymssp.2011.06.012

2.1. Actuator selection

The choice of the actuator was the first important and crucial task of the whole design process as it had relevant influence on the further mechanical design. Many actuators are claimed to be smart and to offer different features. The most important characteristics (Table 1) for this application are efficiency, bandwidth, "passive" mechanical stiffness and compactness (power density).

The knowledge of the magnitude of the machining forces is another critical key issue in choosing the most suitable actuator as in designing the mechanical structure. Authors carried out experimental tests to characterise these forces. By considering all these drivers, the trade-off analysis suggested the high dynamic piezoelectric actuators are the best solution to be implemented in the SP.

2.2. Working principles

The idea of the SP directly derives from the Stewart platform [7], but it has only three degrees of freedom (two rotational around the X and Y axes and one translational along the Z direction) instead of six. The SP has been conceptualised in a modular way both to connect the machine tool spindle with the ram and to support a rotary table. It includes two parts: the fixed platform, directly constrained to the machine tool ram, and the mobile platform, constrained to the housing of the spindle. Three piezoelectric actuators permit the relative movement of these two platforms.

When a displacement is measured at the tool-tip point, three actuators are dynamically activated in order to compensate the vibrations and to smooth their effects out on the workpiece surface. Since a piezoelectric actuator is able to hold on compressive axial loads and to displace in its axial direction, but becomes extremely frail when tensile forces, moments and/or shear forces are applied, special flexible joints and flexures have to be designed to prevent this problem occurring while maintaining high axial and radial stiffness.

The concept of the SP is schematised in Fig. 1, taking into account its flexible configuration (spindle or table). Fig. 2 resumes the SP three-dimensional CAD.

2.3. Mechanical design and prototyping

The SP has to accomplish main functions for a life cycle time of 10 years (32,000 working hours at average frequency):

- to compensate for the chattering vibrations generated at the tool tip point (correction of the tool position up to $\pm 20\,\mu m$),
- to limit the roughness on the workpiece,
- to support the task of the machine without any shape errors.

Table 1
Comparison between different smart actuators.

Actuation method	Efficiency	Speed	Power density	Stiffness
Electro-magnetic	High	Fast	Medium	Low
Electrostatic	High	Fast	Low	Low
Piezoelectric	High	Very fast	High	High
Shape memory	Low	Slow	Very high	Medium
Magnetostrictive	Medium	Medium/fast	Medium/high	High

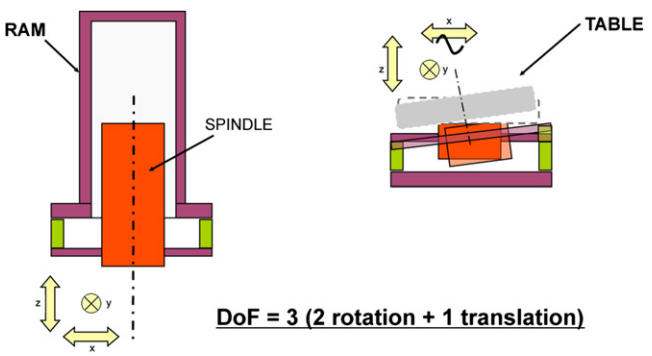

Fig. 1. Working principle applications.

Please cite this article as: F. Aggogeri, et al., Design of piezo-based AVC system for machine tool applications, Mechanical Systems and Signal Processing (2011), doi:10.1016/j.ymssp.2011.06.012

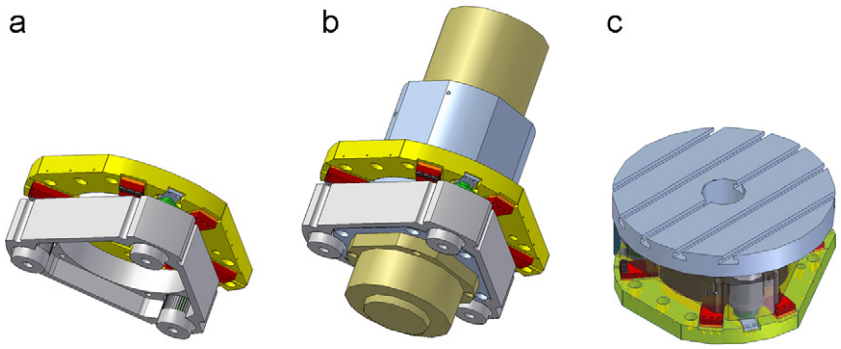

Fig. 2. SP design (a), SP for spindle application (b), SP for Table application (c).

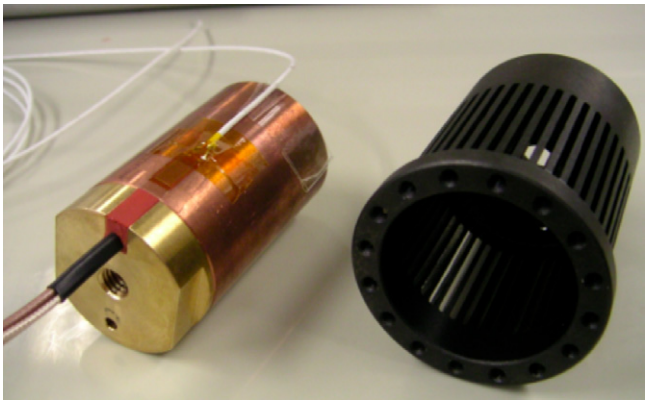

Fig. 3. Design of flexural joint (left); flexural joint and piezo actuator (right).

The SP works in a traditional micromilling environment: temperature close to 40 °C (in any case less than 80 °C), plentiful lubrication and frequency between 100 and 300 Hz.

Every component is designed to accomplish elementary functions. The integration of these functions determines the capability of the system to achieve the technical purposes. Hereafter, the mechanical description of the system is referred to the spindle configuration. The same principles and architecture determine the table configuration.

Referring to Fig. 2, the SP can basically be visualised as an actuation block between two plates interfacing with the machine tool. The fixed plate in aluminium alloy connects directly the SP with the machine tool ram. It houses the actuator extremities as well as one side of the flexural springs. The mobile plate, also made in aluminium alloy, links the SP with the housing of the spindle. It houses the flexural joints as well as the other side of the flexural springs. Three piezoelectric multilayer stack actuators, strategically positioned on the fixed plate (see Fig. 1), permit the relative movement between the two plates.

An electronic device activates the actuators. Applied on the mobile part, a triaxial accelerometer measures the displacements of the tool tip to be converted in the correct voltage for piezo-motion.

The piezoelectric actuators are linked to the fixed plate through the interposition of little plates made by steel. This is necessary for stiffening the connection of the piezoelectric actuators with the (soft) aluminium-alloy platform

A mechanical support system completes the SP, conferring the correct stiffness to the actuator, avoiding undesired stresses and consequent breaks. In fact, every piezo actuator is connected to an innovative flexural joint (Fig. 3), designed to avoid torsional and shear stresses to the piezo elements. Furthermore, two flexural springs are positioned close to every actuator. They have been designed to connect the two plates (fixed and mobile). Every spring is characterised by high torsional and radial stiffness, but free to move in axial direction.

This piezo-stack arrangement embeds also three kinds of sensors to be used for functional and control feedback issues: a force sensor (piezo disk within the stack), a temperature sensor and a displacement (piezo stroke) sensor, called smart disk (Fig. 4).

The smart disk sensor is a patented solution (EP 1857220B1) specifically developed to work with high dynamics and very high precision, without being affected by electro-magnetic field due to the electro spindle.

One side of the bending sensor is fixed to the piezo tip and the opposite is pressed against the flexural joint or the piezo housing (the little steel plate). If the piezo tip is moving, a bending of this spring plate generates a strain signal. This strain

Please cite this article as: F. Aggogeri, et al., Design of piezo-based AVC system for machine tool applications, Mechanical Systems and Signal Processing (2011), doi:10.1016/j.ymssp.2011.06.012

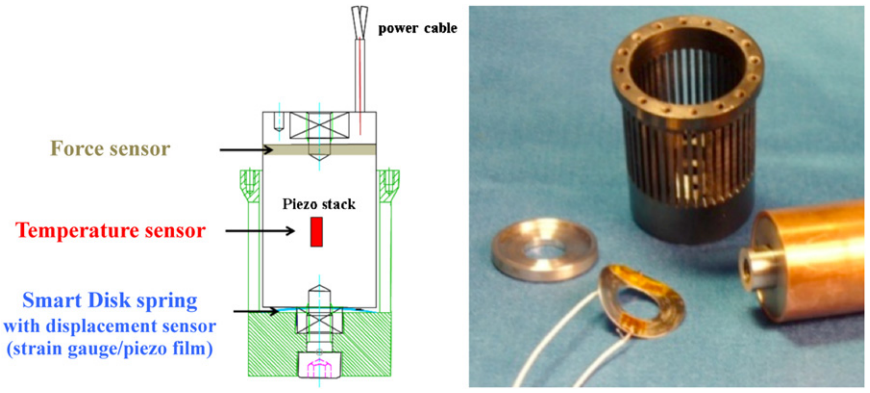

Fig. 4. Smart disk sensor integration (left), piezoelectric actuator, flexural joint and smart disk (right).

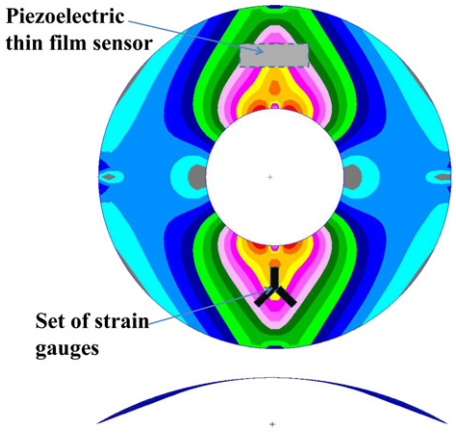

Fig. 5. FE optimisation of smart disk sensor.

signal is acquired by a piezoelectric thin film sensor. In order to validate the piezo film acquisition, strain signals are also measured by a set of strain gauges (redundant configuration).

Electronic components (e.g. amplifiers, signal conditioners) can be integrated like the sensing elements into the smart disk spring as, for example, integrated circuits or MEMS.

The advantages of the smart disk sensor are:

- small size (few mm^3),
- long lifetime and high reliability,
- easiness of application and integration,
- static and dynamic measurements of strain and therefore displacements and/or forces,
- high (submicron) sensitivity,
- possibility to process electrically direct signal.

In order to increase the strain level where the sensors are placed and therefore to obtain a higher precision for the displacement measurement, a suitable configuration for the disk spring was calculated by FE analysis. Fig. 5 shows one of the results of modelling for a stainless steel disk spring with a diameter of 40 mm, 2 mm height, 0.4 mm thickness, simply supported. The maximum strain is approximately 20 μm/m (=20 με) when applying a stroke of 10 μm in the middle of the spring disk. If the stroke is just 1 μm, a strain of 1.6 με is generated which means that theoretically a stroke of 0.1 μm can by measured by the very sensitive piezoelectric thin films (not by the strain gauges, because the minimum strain must exceed 1 με). This dynamic sensitivity has been confirmed by experimental characterisation test on the sensor.

The piezoelectric actuator tip displacement is determined starting from the strains measured on the disk. Then, thanks to the employment of the piezoelectric thin film sensor, the smart disk is able to measure the stroke (in a broadband frequency domain) of the piezo actuator with submicron range sensitivity.

The working conditions can be severe for the piezoelectric actuator; in particular, the working temperature has to be controlled and maintained below 80 °C. For this reason, air fluxes run over the piezo actuator stack through a feeding system placed on the top of every flexural joint. This solution permits the air to flow in the gap between every piezoelectric

Please cite this article as: F. Aggogeri, et al., Design of piezo-based AVC system for machine tool applications, Mechanical Systems and Signal Processing (2011), doi:10.1016/j.ymssp.2011.06.012

actuator and the relative flexural joint. Thus the heat can be removed by forced convection and voided in the external environment thanks to the thin cuts of the flexural joint.

The elements of the SP can be shown in Fig. 6, where depicting photographs of the SP prototype manufacture and assembly can be noted.

2.4. Reliability analysis

When an innovative system is studied, it is fundamental that since the early phases of the design the reliability targets have to be clearly identified [8]. Thus, some analytical efforts are needed, evaluating every potential problem and failure when the product is yet an idea or a drawing. In this way, the design and the realisation of a mechanical system become the result of a structured analytical procedure assessing its quality and reliability [9,10].

Beginning from the morphological–functional decomposition of the SP, Design Failure Mode and Effects Analysis (DFMEA) has been applied. The authors identified every potential failure mode of the elements composing the SP, so as their effects on its functionalities. Following Ford Machinery DFMEA approach, the Risk Priority Numbers (RPNs) have been calculated for every combination of failure cause-mode-effect. Greater is the RPN value, more seriously the potential failure has to be managed [9–11].

It is interesting to determine if the failure should happen during the early beginning of the life cycle (Infant phase) or during the expected operative life (Overall phase). The RPNs detected for the Infant Phase DFMEA are not shown in this paper [11]. They had been reduced by introducing improvement actions on the design process, by reviewing supplier's specifications and material characteristics, and performing Finite Element (FE) analyses. Thus the analytical efforts concentrated on the results of those failures directly related to the product behaviour along the life cycle.

Table 2 resumes the results of DFMEA analysis, listing the most severe RPNs, the relative elements and failure mode. This preliminary analysis shows the piezoelectric actuators (PZT) and the flexural joints (FJ) are the most critical elements, whose reliability characterisation must be deeply investigated. Their functions are extremely related to those of the SP, thus their reliability modelling directly influences the prediction of the entire system behaviour and life cycle time. The innovative flexural joint is a key factor for the functionality of the SP. To predict the reliability behaviour of a component under specified variable working conditions, a deterministic design could fail to provide the necessary understanding. Since the material characteristics are well known and the structural response to mechanical loads is statistically predictable, a probabilistic approach becomes more suitable for this analysis [10,12,13]. A strength–stress analysis is performed to estimate the reliability and the failure rate of the flexural joint [12]. Normal distributions of strength and stress are assumed. The mean value and the standard deviation of strength for the material can be defined by admissible stress multiplied for a coefficient that involves the fatigue. The mean value of stress can be read directly from the results of

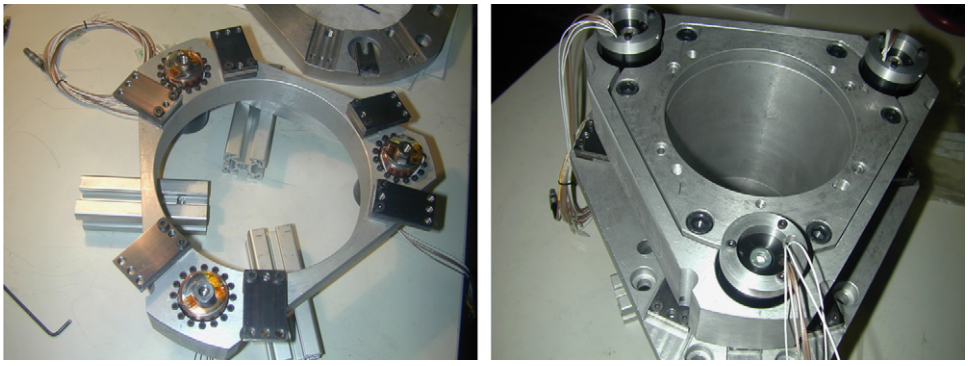

Fig. 6. Manufacturing steps of the SP prototype.

Table 2
DFMEA top RPNs and failure modes.

Element	Failure mode	RPN
Piezo actuator	Break do to fatigue stress	567
Flexural joint	Break do to fatigue stress	441
Accelerometer	Does not properly measure the acceleration (too much overlap noise)	294
Flexural joint	Does not maintain the connection with the mobile platform	280
Flexural joint	Does not maintain the connection with the actuator	245
Piezo actuator	Does not elongate (stroke)/actuate (force) properly	120

Please cite this article as: F. Aggogeri, et al., Design of piezo-based AVC system for machine tool applications, Mechanical Systems and Signal Processing (2011), doi:10.1016/j.ymssp.2011.06.012

the FE analysis after an optimisation of the geometry. The standard deviation of stress has been empirically estimated with reference to the load conditions.

A Safety Margin equal to 4.09 is determined [12]. Under the hypothesis that the strength does not deteriorate with time and the load is applied 120 times per hours, a close to constant failure rate [10,14] of 3.5 failures every million hours is calculated. Consequently, the estimated Mean Time To Failure (MTTF) of the flexural joint is close to 3E05 h, since for constant failure rate λ

$$MTTF = \frac{1}{\lambda} \tag{1}$$

But, looking at DFMEA results, the weakest element of the SP can be the piezoelectric actuator, thus the authors mainly concentrated on its reliability assessment.

As explained before, the actuators are integrated into the SP to compensate the chattering vibrations, displacing in their axial direction to correct the tool tip position. These features addressed the designers to introduce a high voltage PZT (Lead Zirconate Titanate $Pb(Zr,Ti)O_3$ ceramics) multilayer actuator, whose scheme is sketched in Fig. 7.

A multilayer piezoelectric actuator consists of several single thin layers stacked on top of one another. This configuration has the great advantage of achieving high displacement proportional to the applied voltage [15,16].

Applying a voltage up to 1000 V, a cylindrical actuator with height and diameter close to 50 mm can generate in its axial direction a maximum force of 50 kN. A maximum stroke of 55 μm is guaranteed, with an ultrahigh acceleration and response time less than 20 ms.

The piezoelectric cylindrical actuators are able to move in their axial direction, but they are extremely frail when moments and/or shear forces are applied [15,16]. Furthermore, when high voltages are applied to PZT multilayer materials, tensile stresses reduce the durability and stability due to the delamination of layers and electrodes [15,17]. For this reason, the actuators designed for high performances and long durations are preloaded. The preload is an important design issue to increase the resistance to degradation with a negligible loss of the strain output [18]. In the specific case, the piezo stacks are incorporated into a stainless steel casing, compensating tensile stresses up to 6000 N (μ_P close to 4 MPa), where the piezo becomes extremely vulnerable. In this manner, the elements should always work in a compressive state.

There is not a deterministic formulation to assess the lifetime of piezo actuators because many parameters, such as temperature, humidity, voltage, load and preload, operating frequency and material characteristics, concur to determine piezo durability [15,18–21].

Excluding any processing defects [15,16], the reliability characterisation of the three piezo actuators consider their life cycle under the peculiar operating electro-thermal–mechanical conditions of the SP system. It means that both the properties of the ceramic and coupled issues with the device design influence the lifetime of the piezo stack. Thus a complete understanding of the durability must consider the intrinsic failure of the piezo device (function of frequency, voltage and temperature) and the failures derived from undesired torsional, radial or tensile overstresses [16].

Both the supplier and the literature confirm that a high voltage piezo stack actuator (with specified maximum stroke, load and length) should meanly fail after some billions cycles.

Generally, it can be assumed the fatigue lifetime (expressed in cycles) of ferroelectric devices, working at absolute temperature T and under an applied electric field E (V/m), can be described by an empirical rule. The Black's equation (derived from Arrhenius's one),

$$MTTF = aE^{-n}\exp(E_{ac}/kT)*\Gamma\left(1+\frac{1}{\beta}\right) \tag{2}$$

relates the fatigue MTTF to the mechanical–thermal conditions, where a and n are two constants, k is Boltzmann's constant and E_{ac} is a sort of activation energy [15,16,21–24].

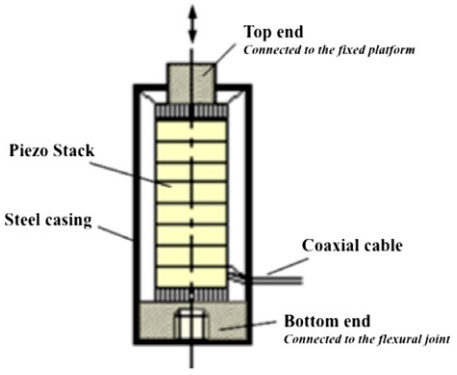

Fig. 7. Scheme of a piezoelectric multilayer actuator.

Please cite this article as: F. Aggogeri, et al., Design of piezo-based AVC system for machine tool applications, Mechanical Systems and Signal Processing (2011), doi:10.1016/j.ymssp.2011.06.012

In the SP, the actuator should work at controlled temperature (meanly 313.15 K) and under an average applied electric field of 2 V/m. Activation energy of 0.99 eV and constant failure rate (β equal to 1) are generally assumed [23]. However, the constant values (a in particular) can vary due to the dimensions and number of the layers, the material and the processing technologies used to assemble the device [22,23]. In order to confirm the accuracy of the quantitative estimation, the authors performed a test campaign. Testing these devices is generally expensive (due to the high purchasing cost) and time-consuming. Looking at these constraints, the authors decided to test only four actuators, accelerating the test at high temperature (373.15 K), anyway respecting the stress limits given by the supplier. During the test, the PZT actuators cycled (frequency equal to150 Hz) with an average electric field E equal to 2 V/m.

The small sample size does not permit accurate estimation of the reliability characteristics. A Weibull distribution (β close to 3 and η equal to 1.1E08 cycles) seemed to be the most appropriate to describe the lifetime of the piezo actuator. The shape parameter β greater than 1 accounted for some wareout.

For the tested piezos, the reliability characteristics, in terms of Mean Time To Failure and B_{10} (the time by which 10% of the elements would fail [10,14]), at high stressing temperature are listed in Table 3. Thus, using the Black's model (Eq. (2)), an acceleration factor

$$A_f = \frac{MTTF_{(T=313.15\,\mathrm{K})}}{MTTF_{(T=373.15\,\mathrm{K})}} \approx 365 \tag{3}$$

has been calculated. By multiplying the results of the test campaign by A_f, it is possible to evaluate the reliability of the tested piezos at standard conditions [10,19].The fatigue life of the piezoelectric actuator at working condition can be described, with a confidence level of 90%, by a MTTF equal to 2.78E10 cycles (51,438 working hours at 150 Hz frequency).

The reliability characterisation of the piezo actuators must comprehend the failures due to overstresses too. The SP has been designed to avoid any kind of undesired stresses on the actuators. Thus, these failure modes are related to the system design and operation, depending on damages that could happen to the elements demanded to prevent them. A failure occurred to the flexural joint or to the couple of flexural springs directly causes the crack of the actuator. Otherwise, tensile overstresses occur when an excessive displacement is needed, exceeding the preload as a consequence.

The strength–stress analysis of the flexural joint assessed the lifetime of the flexural joint is described by a constant failure rate of 3.5 failures every million hours. Furthermore, it is assumed a constant failure rate equal to 5 failures every million hours for every flexural spring.

The probability of failure due to tensile overstress and the relative failure rate is estimated through a stress–strength analysis, following the same approach used for the flexural joint [12]. The calculated Safety Margin is close to 8, meaning this failure source is extremely unlikely, thus its effect is negligible (constant failure rate λ equal to 4.4E−03 failures/mln h).

A Fault Tree Analysis (FTA) can be a useful tool to resume the design for reliability issues, providing useful information about the likelihood of a failure (top event) occurring due to different causes [10,11]. The failure of the actuator depends on different sources; for every potential cause of failure (FC), the estimated MTTF is listed in Table 4. The authors used these data in order to build the Fault Tree logic and obtain the actuator failure (top-event).

By combining the probability of failure due to different sources, every piezoelectric multistack actuator shows a reliability of 0.977 after 2 years, decreasing to 0.875 after 10 years. The estimated B_{10} is equal to 25,886 h. The piezo device seemed to hold enough satisfactory reliability characteristics to accomplish the SP functions along the 10 years life cycle.

Table 3
Reliability characteristic of piezo actuators at stressed temperature.

Reliability characteristics	Value (cycles)
B_{10}	5.17E07
MTTF	9.78E07
MTTF (1S c.b. 90%)	7.61E07

Table 4
Likelihood of causes generating piezo failure.

Type	Source	MTTF (working h)
FC1	Intrinsic failure due to fatigue	5.15E04
FC2	Break of the flexural joint	2.86E05
FC3	Break of the flexural springs	2.00E05 each
FC4	Tensile overstress	2.48E08

Please cite this article as: F. Aggogeri, et al., Design of piezo-based AVC system for machine tool applications, Mechanical Systems and Signal Processing (2011), doi:10.1016/j.ymssp.2011.06.012

3. Mechatronic models and control

3.1. The mechatronic model

The complexity of compensating the vibrations through an active control system is reflected on the advanced control algorithm needed. The SP implies several issues that have to be solved simultaneously, embracing different engineering fields (structural, electrical, signal processing, control, thermal, etc.): a real complex mechatronic problem.

A test bench configuration has been designed, where the SP is constrained to a flange (Fig. 8). The flange is fixed to the ground by means of three legs of changeable extension. This solution permits to change the stiffness of the frame, introducing different eigenfrequencies of the system. The basic idea behind the design of the test bench is to reproduce, at least partially, the dynamic behaviour of a machine tool.

A FE model has been developed in order to optimise the design. Experimental tests (static and dynamic) were carried to validate this model. The validation is needed as the FE model has been used to develop a model-based control.

The FE model consists of approximately 170,000 elements. It includes 3D solid elements (Brick and Tetra) to model main building block of the SP (i.e. plates, spindle, joints, supporting legs), 2D shell elements to model the flexures and one-dimensional elements (with stiffness and damping parameter) to model the piezoelectric actuators (Fig. 8).

The full test bench model has been reduced following the Craig and Bampton procedure [25]. The modes and frequencies of the complete and reduced model are shown in Table 5.

The reduced finite element model has been imported in Matlab/Simulink environment to perform several dynamic simulations, testing and checking different control algorithms. The generic reduced mechanical system is completely described by

$$[M]\ddot{z}+[V]\dot{z}+[K]z=F \tag{4}$$

where z is the vector of displacements of physical DOFs, F the vector of forces, $[M]$ and $[K]$ the positive definite mass and stiffness matrices and $[V]$ the symmetric damping matrix. The dynamics of a system is often described in a state space form, as it is easier to handle for control purposes:

$$\begin{aligned}\dot{x}&=[A]x+[B]u \quad \text{with } x=\begin{Bmatrix}\dot{z}\\ z\end{Bmatrix}\\ y&=[C]x+[D]u \quad \text{with } u=\begin{Bmatrix}F\\ 0\end{Bmatrix}\end{aligned} \tag{5}$$

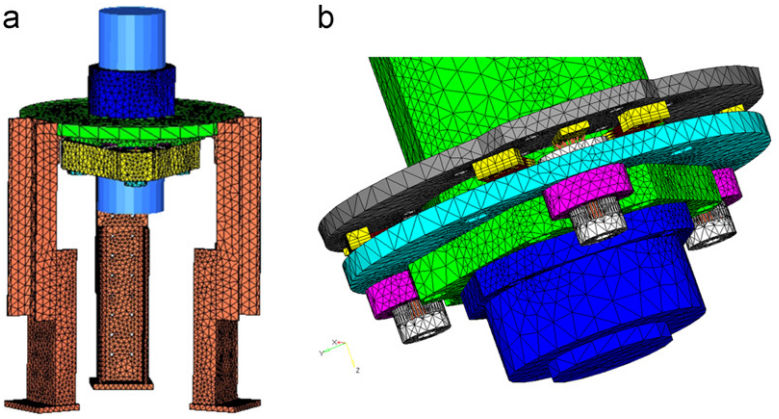

Fig. 8. Finite element model of the whole test bench (a) and a detailed view (b).

Table 5
Mode frequencies of the complete FE model and reduced model.

Mode	FE complete (Hz)	Reduced (Hz)	Difference (%)
1	78.9	77.9	1.2
2	79.6	78.4	1.5
3	191.8	190.9	0.5
4	209.8	206.9	1.3
5	213.2	213.2	0
6	310.8	310.3	0.16
7	558.3	561.8	0.62

Please cite this article as: F. Aggogeri, et al., Design of piezo-based AVC system for machine tool applications, Mechanical Systems and Signal Processing (2011), doi:10.1016/j.ymssp.2011.06.012

with

$$A=\begin{bmatrix} -[M]^{-1}[V] & -[M]^{-1}[K] \\ [I] & [0] \end{bmatrix}, \quad B=\begin{bmatrix} [M]^{-1} \\ [0] \end{bmatrix} \tag{6}$$

and $[C]$ and $[D]$ depends on the chosen outputs, while x and u are, respectively, the state vector and the force input vector.

3.2. Piezoelectric actuator linear model

The piezoelectric actuators must be included into the reduced model. In this paper, the linear model of the piezoelectric actuator is shortly addressed, lacking in any treatment about hysteresis [26–28].

Generally, a piezoelectric stack is assumed to strain in only one direction. Thus, the constitutive equations for a one-dimensional excitation and deformation of a piezoceramic element [28] are

$$D=\varepsilon^T E+dL \tag{7}$$

$$S=dE+s^E L \tag{8}$$

where D is the electric density or flux density (C/m^2); E the electric field (V/m); L the mechanical stress (N/m^2); S the mechanical strain (m/m); ε the dielectric permittivity of the material ($F/m=C^2/N\,m^2$); d the piezoelectric d-constant ($m/V=C/N$); and s the mechanical compliance (inverse of Young's modulus) (m^2/N).

All these parameters are either related to (or a function of) the direction of the mechanical or electrical excitation. For example, the value of the d-constant may change as it is expressed as d_{33}, d_{31}, d_{15}, etc. Then, following the use of subscripts and superscripts in piezoelectricity, Eqs. (7) and (8) defined for a piezoelectric stack, are expressed more specifically as

$$D_3=\varepsilon_3^T E_3+d_{33}L_3 \tag{9}$$

$$S_3=d_{33}E_3+s_3^E L_3 \tag{10}$$

From the above maths relations, it can be demonstrated that the constitutive equations for the piezoelectric stack are the following:

$$Q_{pzt}=C_{pzt}V_{pzt}-d_{33}L_3 \tag{11}$$

$$X_{pzt}=d_{33}V_{pzt}-\frac{1}{k_a}F_{pzt} \tag{12}$$

where k_a is the stiffness of the piezoceramic stack, F_{pzt} the actuation force, x_{pzt} the stroke, Q_{pzt} the charge and V_{pzt} the applied voltage. Eq. (12) represents the linear model of the piezoelectric actuator to be embedded inside the reduced model. Furthermore, for the operation of the stack under the maximum voltage allowed, V_{max}, Eq. (12) can be rearranged in the form:

$$F_{pzt}=-k_a X_{pzt}+k_a d_{33}V_{max} \tag{13}$$

3.3. The LQG-H_2 controller

The control chosen for this simulation is based on the H_2 theory, due to its wide literature spread and its applications for AVC problems [29–33]. The control chain starts with the signal provided by the triaxial accelerometer, placed on the mobile platform. A control digital board is obviously needed in order to process data from the sensor and elaborate the driving signals to the three piezoelectric actuators (Fig. 9).

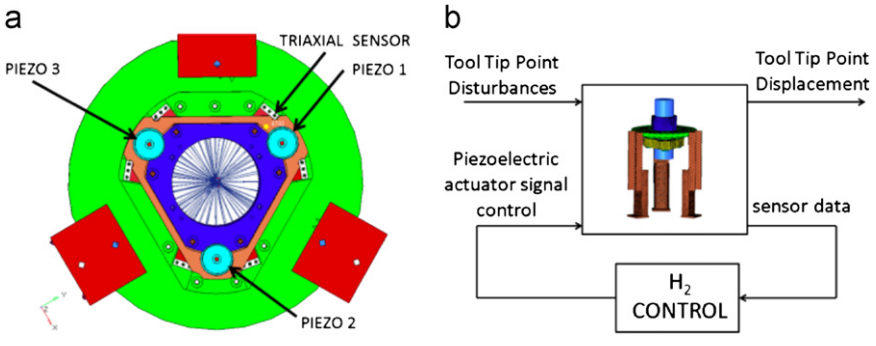

Fig. 9. Bottom view of the test bench with the position of the piezo actuators and the triaxial sensor highlighted (a) and control H_2 scheme (b).

Please cite this article as: F. Aggogeri, et al., Design of piezo-based AVC system for machine tool applications, Mechanical Systems and Signal Processing (2011), doi:10.1016/j.ymssp.2011.06.012

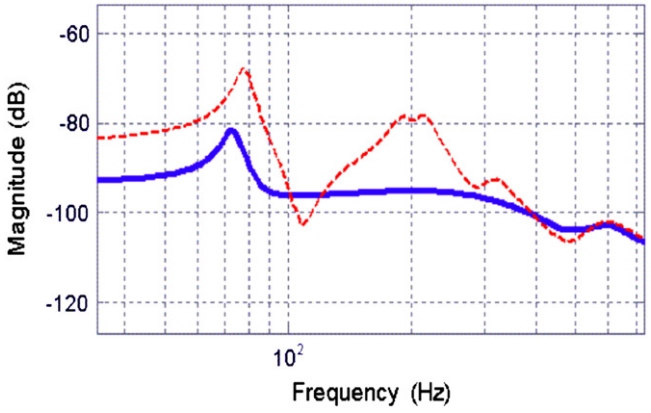

Fig. 10. FRFs of the TTP: *X* displacement versus *X* force input (continuous line—closed loop , dashed line—open loop).

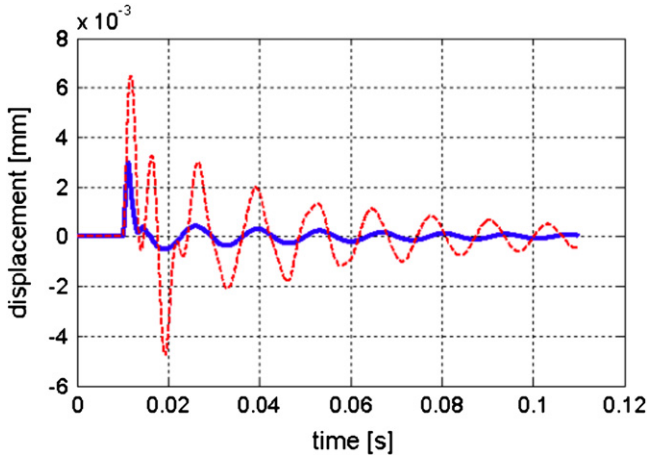

Fig. 11. System response after an impulse at TTP: *X* displacement of TTP after being excited along *X* direction (continuous line—closed loop, dashed line—open loop).

The dynamic system, as described by Eq. (5), may be partitioned as

$$\begin{aligned} \dot{x} &= Ax + B_1 w + B_2 u \\ z &= C_1 x + D_{12} u \\ y &= C_2 x + D_{21} w \end{aligned} \tag{14}$$

where x is the state vector, u the control vector, $w^T = [v_u^T \; v_y^T]$ the exogenous input, z the regulated variable (displacement of the tool tip point), y the measured output (signals from the sensor) and v_u and v_y are process and measurement noises. The noises are supposed to be uncorrelated. The H_2 control problem consists in finding a realisable controller dynamic system, such that $\|G_{wz}\|_2$ is minimal, where

$$z(s) = G_{wz}(s) w(s) \tag{15}$$

The H_2 dynamic controller assumes the following form:

$$\begin{aligned} \dot{\bar{x}} &= (A - B_2 K_c - K_e C_2)\bar{x} + K_e y \\ u &= -K_c \bar{x} \end{aligned} \tag{16}$$

where K_e and K_c are solutions of the Filter Algebraic Riccati Equation (FARE) and Control Algebraic Riccati Equation (CARE) [29].

Following the former equations an H_2 control algorithm has been derived. It is able to significantly suppress the oscillation amplitude of the Tool Tip Point of the spindle as shown in Figs. 10 and 11. The results refer to the *X*–*Y* plane, orthonormal to the spindle axis. The shape of the excitation impulse is a time window of 1 ms width and 200 N amplitude.

In particular, Fig. 10 reports the FRFs of the spindle TTP while Fig. 11 shows the response time of the system after being excited by an impulse in closed and open loop.

Please cite this article as: F. Aggogeri, et al., Design of piezo-based AVC system for machine tool applications, Mechanical Systems and Signal Processing (2011), doi:10.1016/j.ymssp.2011.06.012

4. Conclusion

The robust mechatronic design of the SP enables the piezoelectric actuators to work properly, ensuring the achievement of maximal and enduring performances. The simulation results show an appreciable decrease of the oscillation of the TTP, thus confirming the validity of working principle. It is possible to significantly suppress the oscillations of the TTP using the proposed control scheme: a sensor placed on the mobile platform, an H_2 control scheme and three piezoelectric actuators fed by a dedicated electronic board. The results are very promising also due to the robustness of the SP design, providing the piezo-based system to work efficiently and safely throughout the life cycle of the machine. On the other hand the SP is a modular solution, employable for table application or spindle-damping application.

Furthermore, the effectiveness of the SP at high frequencies, excited typically by the high speed micromilling cutters (multi-tooth) is ensured by the high inherent stiffness of the devices and selecting proper adaptive control strategies (e.g. the "repetitive" controller) for narrow band forced vibrations. A bandwidth up to 2 kHz for the proposed SP can be reasonably achieved.

The future steps foresee the physical realisation of the test bench and the final experimental tests in order to validate completely the numerical model and the control algorithm. For the time being, the results showed in this paper demonstrate the potential of the SP in suppressing the vibration of machine tools. Therefore, the proposed SP can represent a great challenge in machine tools sector and open interesting perspectives for industrial applications of adaptronic within this field.

Acknowledgements

The work carried out in this paper is partially funded by the EU Project (CP-FP-213999-2) "ADAMOD" (Plug-in Adaptronic Modules for real-time errors (Thermal & Vibration) compensation and superfine positioning in reconfigurable high precision) machine tools). The authors do wish to thank all the partners of the consortium.

References

[1] J. Tlusty, M. Polacek, The stability of machine tools against self excited vibrations in machining, ASME International Research in Production Engineering 1 (1963) 465–474.
[2] S.A. Tobias, Machine Tool Vibration, Blackie, London, UK, 1965.
[3] Y. Altintas, A Woronko, A Piezo Tool, Actuator for precision turning of hardened shafts, CIRP Annals—Manufacturing Technology 51 (1) (2002) 303–306.
[4] B. Denkena, O. Gümmer, C. Will, F. Hackelöer, Compensation of static and dynamic tool deflections during milling processes by an adaptronic spindle system, in: Proceedings of the 2nd International Conference on Innovative Cutting Processes & Smart Machining, Cluny, France, 2008.
[5] W.G. Drossel, V. Wittstock, Adaptive spindle support for improving machining operations, CIRP Annals—Manufacturing Technology 57 (1) (2008) 395–398.
[6] P. Radecki, W. Kruse, A. Welsh, E. Moro, G. Park, M. Bement, Improving a turning process using piezoelectric actuators, in: Proceedings of the IMAC-XXVII, Orlando, FL, 2009.
[7] I. Abi Hanieh, A. Preumont, N. Loix, Piezoelectric stewart platform for general purpose active damping interface and precision control, in: Proceedings of the European Space Mechanisms and Tribology Symposium, Liege, Belgium, 2001.
[8] N. Bernstein, Reliability analysis techniques for mechanical systems, Quality Reliability Engineering International 1 (4) (1985) 235–248.
[9] D.H. Stamatis, Failure Mode and Effect Analysis, ASQ Quality Press, Milwaukee, WI, 1995.
[10] M. Pecht, Product Reliability, Maintainability, and Supportability Handbook, CRC, New York, NY, 1995.
[11] M. Mazzola, F. Aggogeri, A. Merlo, B. Brunner, M. De la O. Rodriguez, Reliability characterization of a piezoelectric actuator based AVC system, in: Proceedings of the 10th ASME Biennial Conference on Engineering Systems Design and Analysis, Istanbul, Turkey, 2010.
[12] A.D.S. Carter, Mechanical Reliability, Macmillan, London, UK, 1986.
[13] K.G. Swift, M. Raines, J.D. Booker, Advances in probabilistic design: manufacturing knowledge and applications, Journal of Engineering Manufacture—Part B 215 (2001) 297–313.
[14] Reliasoft Corp., Life Data Analysis Reference, Reliasoft Publishing, Tucson, AZ, 2005.
[15] J. Pritchard, C.R. Bowen, F. Lowrie, Multilayer actuators: review, British Ceramic Transactions 100 (6) (2001) 1–9.
[16] K. Uchino, Ferroelectric Devices, CRC Press, Boca Raton, FL, 2000.
[17] D.A. Van den Ende, B. Bos, W.A. Groen, L.M.J.G. Dortmans, Lifetime of piezoceramic multilayer actuators: interplay of material properties and actuator design, in: Proceedings of the International Conference on Electroceramics, Arusha, Tanzania, 2007.
[18] P.M. Chaplya, M. Mitrovic, G.P. Carman, F.K. Straub, Durability properties of piezoelectric stack actuators under combined electro-mechanical preload, Journal of Applied Physics 100 (2006) 124111.
[19] K. Nagata, S. Kinoshita, Relationship between lifetime of multilayer ceramic actuator and temperature, Japanese Journal of Applied Physics 34 (1995) 5266–5269.
[20] T. Sakai, H. Kawamoto, Durability properties of piezoelectric stack actuator, Japanese Journal of Applied Physics 37 (1998) 5338–5341.
[21] J. Thorengrueng, T. Tsuchiya, K. Nagata, Lifetime and degradation mechanism of multilayer ceramic actuator, Japanese Journal of Applied Physics 37 (1998) 5306–5310.
[22] K. Uchino, Materials issues in design and performance of piezoelectric actuators: an overview, Acta Materialia 46 (11) (1998) 3745–3753.
[23] J.H. Koh, T. Kim, Reliability of $Pb(Mg,Nb)O_3$–$Pb(Zr,Ti)O_3$ multilayer ceramic piezoelectric actuators by Weibull method, Microelectronics Reliability 46 (2006) 183–188.
[24] P. Pertsch, S. Richter, D. Kopsch, N. Krämer, J. Pogodzik, E. Henning, Reliability of piezo-electric multilayer actuator, in: Proceedings of the Actuator 2006 Conference, Bremen, Germany, 2006.
[25] R.R. Craig, M.C.C. Bampton, The coupling of substructures for dynamic analyses, AAIA6 7 (1968) 1313–1319.
[26] M. Goldfarb, N. Celanovic, A Lumped, Parameter electromechanical model for describing the nonlinear behavior of piezoelectric actuators, Transactions of the ASME 119 (1997) 478–485.
[27] V. Giurgiutiu, S.E. Lyshevski, Micromechatronics, CRC Press, Boca Raton, FL, 2004.
[28] IEEE Standard on Piezoelectricity, ANSI/IEEE Std 176-1987, 1988.
[29] W.K. Gawronski, Advanced Structural Dynamics and Active Control of Structures, Springer, New York, NY, 2004.

Please cite this article as: F. Aggogeri, et al., Design of piezo-based AVC system for machine tool applications, Mechanical Systems and Signal Processing (2011), doi:10.1016/j.ymssp.2011.06.012

[30] K. Zhou, J.C. Doyle, Essentials of Robust Control, Prentice-Hall, 1998.
[31] C. Robl, G. Englberger, G. Farber, H2-Control with acceleration feedback for a micro positioning system, in: Proceedings of the 1999 IEEE International Conference on Control Applications, 1999, pp. 187–192.
[32] M. Zapateiro, H.R. Karimi, N. Luo, B.M. Phillips, B.F. Spencer Jr. A mixed H2/H∞-based semiactive control for vibration mitigation in flexible structures, in: Joint 48th IEEE Conference on Decision and Control and 28th Chinese Control Conference, 2009, pp. 2186–2191.
[33] G. Foutsitzi, D.G. Marinova, E. Hadjigeorgiou, G.E. Stavroulakis, Robust H2 vibration control of beams with piezoelectric sensors and actuators, in: 2003 International Conference on Physics and Control, 1 (PHYCON'03), 2003, pp. 157–162.

Please cite this article as: F. Aggogeri, et al., Design of piezo-based AVC system for machine tool applications, Mechanical Systems and Signal Processing (2011), doi:10.1016/j.ymssp.2011.06.012